# EXPERIMENTAL STUDY ON THE MECHANISM FOR WATER INFILTRATING INTO AN AIR BLOCK AREA

MENG, L.[1,2] – ZHAO, G.[3] – ZHANG, C.[3*] – WANG, L.[3] – XU, Y.[3]

[1]*School of Water Resources and Environment, China University of Geosciences, Beijing 100083, China*

[2]*Institute of Hydrogeology and Environmental Geology, Chinese Academy of Geological Sciences, Shijiazhuang 050061, China*

[3]*College of Geosciences and Engineering, North China University of Water Resources and Electric Power, Zhengzhou 450046, China*

**Corresponding author*
*e-mail: hydrozcy@163.com; phone: +86-186-3900-6624*

(Received 23rd Feb 2019; accepted 3rd May 2019)

**Abstract.** Gas is usually ignored in traditional studies of water movement processes in the vadose zone. However, a large number of simulation experiments show that gas is an important factor effecting water movement. In this paper, a two-dimensional sand tank model is built to observe the changes of gas pressure and negative pressure during rainfall events with different intensities and boundaries and investigate the interaction between gas and water to reveal the block effect of gas on water movement. The results show three main effects of gas affecting water infiltration. Firstly, the water infiltration causes the gas pressure increased, which results in the decrease of unsaturated hydraulic conductivity. Secondly, the gas will escape to surroundings even break through the overlying saturated layer if the infiltration causes the gas pressure to increase to a critical value. The movement of gas in the vadose zone is mainly in vertical under the condition of gas insulation boundary, while in both vertical and horizontal under the condition of gas exhaust boundary. Finally, according to the variations of gas pressure with depths in the central profile, the vadose zone is divided into three zones: gas escaping zone, gas pressure fluctuating zone and gas pressure fast-decreasing zone.
**Keywords:** *sand tank, rainfall intensity, gas pressure, infiltration, physical experiments, moisture content*

## Introduction

Gas flow is usually ignored in research into water movement processes in the vadose zone, and it is generally assumed that gas can freely discharge or invasive, so the gas pressure and atmospheric pressure are balanced (Peng, 2002). In fact, water movement in the vadose zone is the result of the mutual displacement of gas and water in the vadose zone pores, especially during events of heavy rainfall infiltration and pressured water infiltration. Water infiltration causes the gas to be constantly compressed under the weight of water and the gas cannot dissipate within a short time period, resulting in an increase in gas pressure and a reduction in the infiltration rate (Jarrelt, 1978; Lei, 1988; Lu, 1994).

It was found that the water infiltration rate was smaller under gas insulation conditions than under free exhaust conditions, and that gas will break through the overlying layer to escape when the pressure reaches a breakthrough value in the one-dimensional soil column infiltration experiment (Wang, 1997). Others had also come to this conclusion (Peck, 1965; Toma, 1986; Grismerand, 1994. Weir and Kissling divided the soil column into three regions to describe the water phase and gas phase: an upper


http://www.aloki.hu ● ISSN 1589 1623 (Print) ● ISSN 1785 0037 (Online)
DOI: http://dx.doi.org/10.15666/aeer/1704_78377853

layer, a transition layer and a lower layer. Water-gas phase interactions mainly occur in the transition layer, where the existence of gas will affect the water penetration coefficient. Peng et al. (2002) found that the water infiltration rate obviously declined when the air flow rate at the bottom of the soil column was controlled instead of exhausting freely in a one-dimensional two-phase flow experiment. The flow movement to ambient infiltration zone and surface is due to gas pressure persistent arise and gas displacement by water is the main characteristic in infiltration process (Lei, 2009). Ghosh et al. (2012) made an experimental investigation on vertical gas–liquid counter-current two-phase flow and obtained nonlinear relationships between the developed flow regimes and input parameters. Jie et al. (2013) illustrated the essential of consideration of gas resistance. It was found that the calculated infiltration time considering gas resistance term in the stratified hypothesis model agrees with the measured value with low deviation degree and a very small fluctuation. Herrada et al. (2014) proposed a model to simulate infiltration into heterogeneous soils, with arbitrary initial water content distributions, subject to unsteady rainfall, and under the free draining condition. Li et al. (2015) obtained the results that the channel differential pressure on both sides brings obvious fluctuations when the liquid is infiltrated. It is the gas flow rate not the amount of liquid infiltration affects the fluctuation significantly in the amplitude of the pressure differential. Du et al. (2017) analyze the mechanisms of soil water and vapour transport in the desert vadose zone using the Hydrus-1D model. Xiao et al. (2018) created an artificial-intelligence system that identifies nanofluid gas-liquid two-phase flow states in a vertical mini-channel. Min et al. (2018) investigated the groundwater recharge and seepage velocity in the deep vadose zone under typical irrigated agricultural land-use types.

Most researchers focus on one-dimensional soil column infiltration experiments, studying the effect of the presence of gas in the vadose zone by controlling the air flow rate at the bottom of the column, with little consideration given to the existence of the overlying aquifer. Although pressure changes under infiltration conditions are analysed, the relationship between air pressure and moisture content are not presented. Research of two-dimensional problems of rainfall infiltration is relatively barely (Zhao, 2011). In this paper, based on a two-dimensional physical model, experiments are designed to investigate rainfall infiltration processes under conditions of four different rainfall intensities and two different boundaries. That the changes of gas pressure and the hydrodynamic filed under different rainfall intensities and boundaries are investigated. The gas pressure on the profile along the central line and at three typical points is chosen to make data analysis. The relationship between negative gas pressure and moisture content is also analysed.

## Methods

### *Experimental equipment*

The experimental equipment comprises a sand tank, a rainfall simulator and a rainfall collector, shown in *Figure 1*. The size of the sand tank is 130 cm × 120 cm × 30 cm. The rainfall simulator is a plate with circular holes (diameter is 0.2 mm). The size of the rainfall simulator is 50 cm × 30 cm × 20 cm.

The sand tank is the main body of the test device. It is made of a high-quality, water-resistant wood-based material, with a metal box at the bottom forming the saturated zone. The tank is fitted with intake pipes, drainage pipes and piezometric tubes.


http://www.aloki.hu ● ISSN 1589 1623 (Print) ● ISSN 1785 0037 (Online)
DOI: http://dx.doi.org/10.15666/aeer/1704_78377853

Because the tank is symmetrical, so 19 gas pressure sensors (measuring range: -1000~1000 Pa; resolution: ±0.25% FS; manufacturer: Chang'an University and Huarui Transducer Technology Company) are installed in the front side of the sand tank, and 17 negative pressure sensors (measuring range: 0~-50 kPa; resolution; ±0.25%FS; manufacturer: Chang'an University and Huarui Transducer Technology Company) are installed in the back side of the sand tank. The effective rainfall simulation zone is 50 cm × 30 cm on the top of the setup. The experimental medium filled in the tank is silty sand. The joint parts of the device are well sealed to prevent water from flowing out of the device. Several air outlets with a diameter of 1 cm are installed at not only the left side but also the right side of the device for free exhaust. The origin of the coordinate system is at the left-bottom corner of the sand tank. The X axis increases positively to the right, and the Z axis increases positively upwards, so the coordinate of each pressure observation point is obtained. A markovian bottle is used to keep the phreatic level at 25 cm considering the base level at X axis.

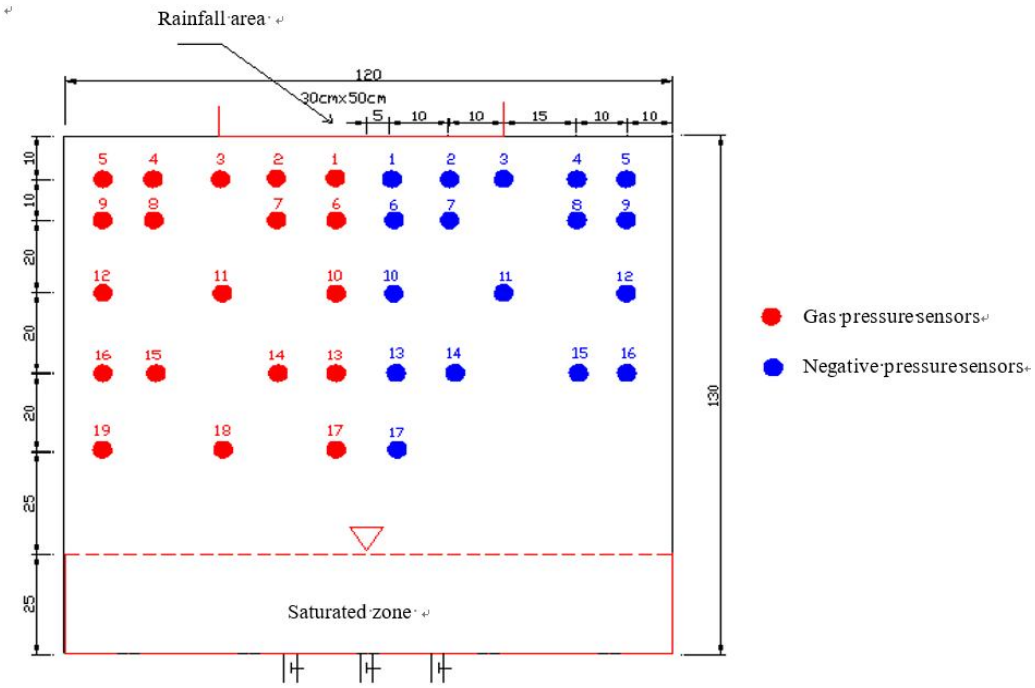


***Figure 1.*** *Schematic diagram of experimental setup*

## *Experimental design*

In order to analyze the affecting factors on water–gas phase flow migration law in the vadose zone, several different rainfall intensities and two different boundaries are set in the experiments. Two different boundaries are gas insulation condition and free exhaust condition. Gas insulation condition is that both the left and right boundaries of the sand tank model are closed and gas cannot be discharged (zero flux boundary). Free exhaust condition is that both the left and right sides of the sand tank model are partly open (flux boundary). The detailed experimental design is shown in *Table 1*. The rainfall duration is 30 min in each experiment. The groundwater level of saturated zone is kept at 25 cm. In each experiment, the negative gas pressure (matric potential) and the gas pressure and moisture content are measured and recorded continually.


http://www.aloki.hu ● ISSN 1589 1623 (Print) ● ISSN 1785 0037 (Online)
DOI: http://dx.doi.org/10.15666/aeer/1704_78377853

***Table 1.*** *The experimental design*

| Research content | Boundary | Rainfall intensity (cm/h)/ amount of rainfall (cm) |
|---|---|---|
| Changes of the aerodynamic field | Gas insulation condition | 58/29 |
| | Free exhaust condition | 53/26.5 |
| Changes of the gas pressure with the depth | Free exhaust condition | 65/32.5 |
| | Gas insulation condition | 58/29; 40/20; 20/10 |
| Changes of gas pressure at typical points | Gas insulation condition | 78/39; 20/10 |
| Changes of the hydrodynamic field | Gas insulation condition | 58/29; 20/10 |
| Distributions of moisture content in the central profile | Gas insulation condition | 78/39; 20/10 |
| Relationship between the gas phase and the water phase | Gas insulation condition | 58/29; 20/10 |

## Experimental results

### *Changes of the aerodynamic field under different boundaries*

Distributions of the gas pressure field with a rainfall intensity of 58 cm/h (gas insulation boundary, presented in grey solid lines) and 53 cm/h (free exhaust boundary, presented in grey dotted lines) at different rainfall durations are shown in *Figures 2* and *3* respectively. The time varying maximum gas pressure of the central profile at X = 60 cm under different boundary conditions are presented in *Figure 4*.

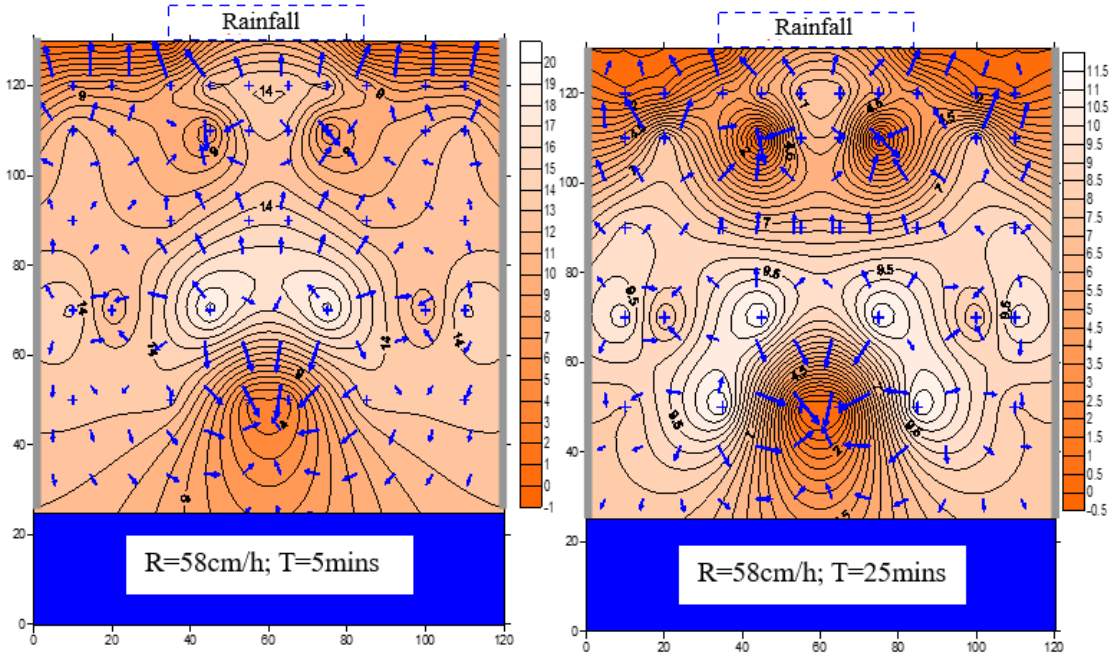


***Figure 2.*** *Gas pressure distributions for a rainfall intensity of 58 cm/h (left: the rainfall duration is 5 min; right: the rainfall duration is 25 min; unit of gas pressure: Pa)*


http://www.aloki.hu ● ISSN 1589 1623 (Print) ● ISSN 1785 0037 (Online)
DOI: http://dx.doi.org/10.15666/aeer/1704_78377853

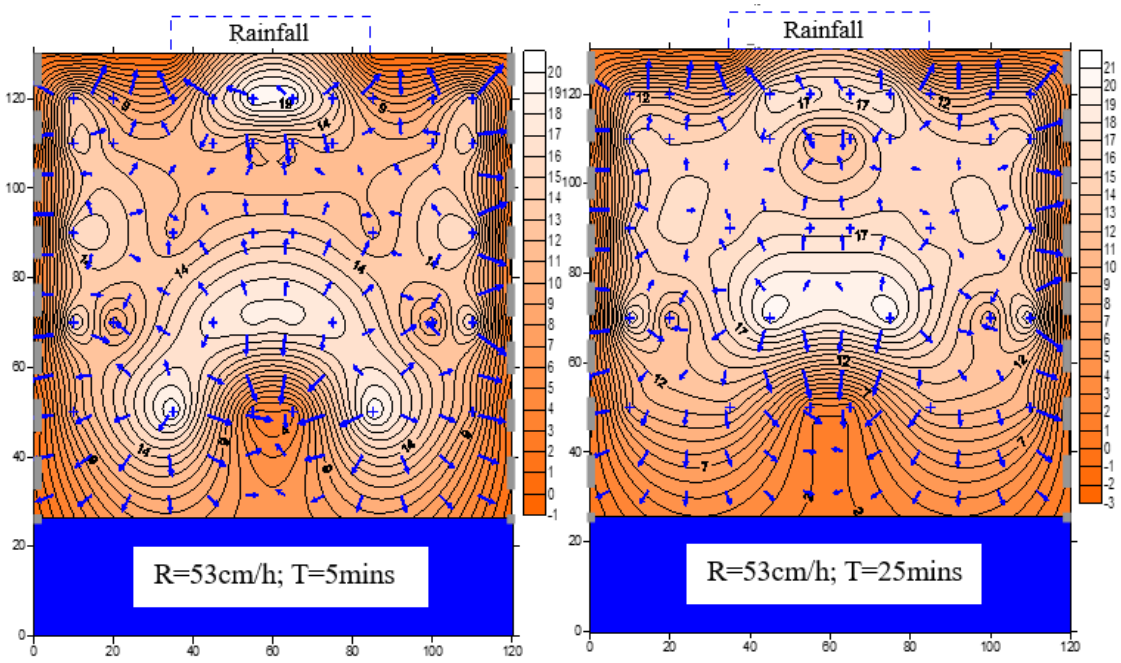


***Figure 3.*** *Gas pressure distributions for a rainfall intensity of 53 cm/h (left: the rainfall duration is 5 min; right: the rainfall duration is 25 min; unit of gas pressure: Pa)*

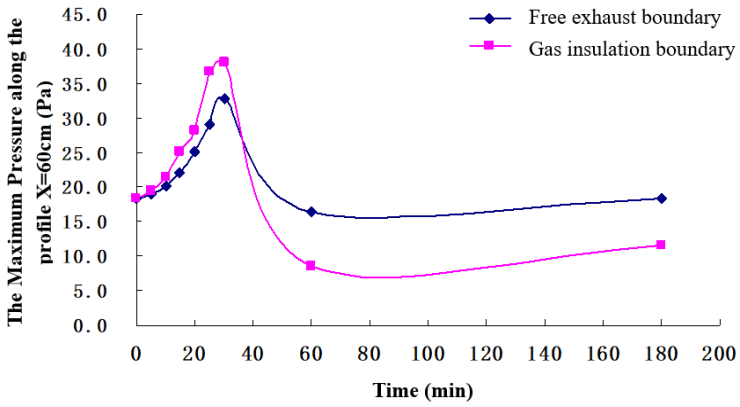


***Figure 4.*** *The time varying of the maximum gas pressure of the central profile at X = 60 cm under different boundary conditions*

### *Changes of the gas pressure with the depth*

Take the gas pressure at the central profile along X = 60 cm for example, the time-varying relationships between the gas pressure and depth in the vadose zone under different rainfall intensities and rainfall durations are shown in *Figure 5*. The rainfall duration is 0, 11, 20, 26 min respectively for each line in each figure.

### *Changes of gas pressure at typical points*

Three gas pressure observation points at different locations in the vadose zone are selected. The first point (1#) locates at the rainfall area. The second point (3#) locates at


http://www.aloki.hu ● ISSN 1589 1623 (Print) ● ISSN 1785 0037 (Online)
DOI: http://dx.doi.org/10.15666/aeer/1704_78377853

the front of rainfall area and non-rainfall area. The third point (5#) locates at non-rainfall area. The changes of gas pressure values of the above three points are plotted in *Figure 6*.

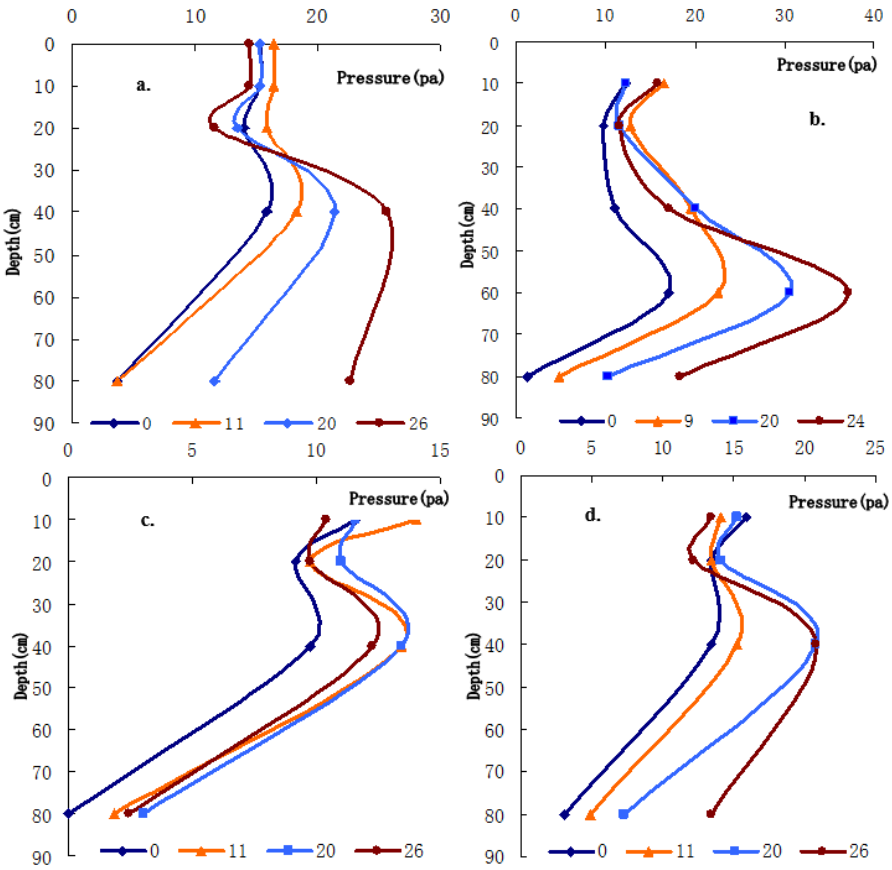


***Figure 5.*** *Relationship between gas pressure and depth in the vadose zone for different rainfall intensities and different rainfall durations (a: rainfall intensity is 65 cm/h; b: rainfall intensity is 58 cm/h; c: rainfall intensity is 40 cm/h; d: rainfall intensity is 20 cm/h)*

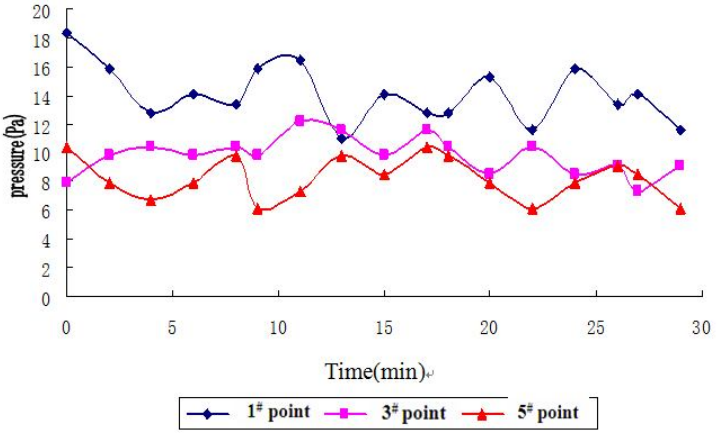


***Figure 6.*** *Gas pressure variations with time at different observation points (1# point is located at the rainfall area; 3# point is located at the front of rainfall area and non-rainfall area; 5# point is located at the non-rainfall area)*


http://www.aloki.hu ● ISSN 1589 1623 (Print) ● ISSN 1785 0037 (Online)
DOI: http://dx.doi.org/10.15666/aeer/1704_78377853

The changes of gas pressure with time under different rainfall intensities are shown in *Figure 7*. It shows that the pressure fluctuates constantly around a mean value during a rainfall event. The mean value is 12.65 Pa when the rainfall intensity is 20 cm/h, while the mean value is 16.24 Pa when the rainfall intensity is 78 cm/h. The mean value of the pressure is greater when the rainfall rate is 78 cm/h than that when the rainfall rate is 20 cm/h. This proves that rainfall intensity has an important effect on the changes in gas pressure in the vadose zone.

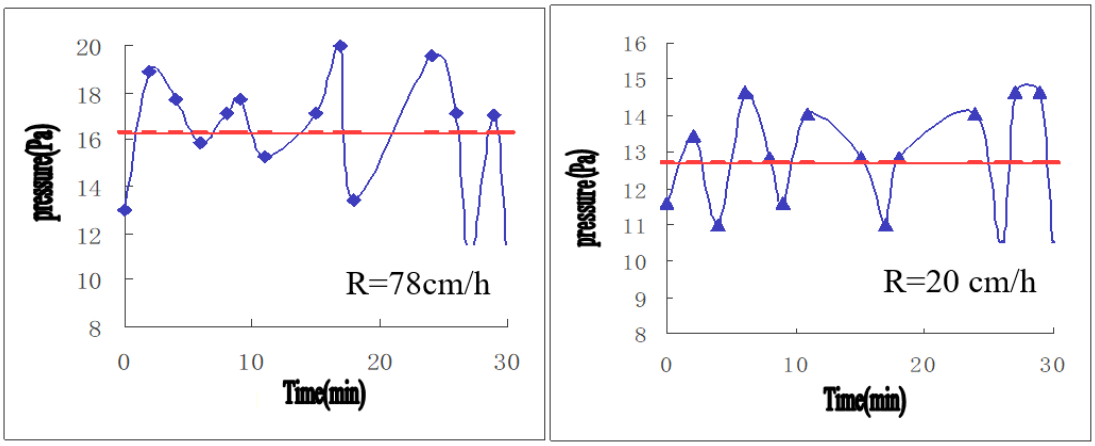


***Figure 7.*** *Gas pressure variations with time in the vadose zone under different rainfall intensities*

Fluctuations in gas pressure are mainly related to unevenly distributed rainfall, surface disturbance, and the density of the experimental medium. These factors led to a change in the hydrodynamic field in the vadose zone, and to gas pressure fluctuations. It can be concluded that the water and gas phases are closely linked in the vadose zone and the mutual displacement processes should not be ignored.

### *Changes of the hydrodynamic field*

The distributions of hydrodynamic fields under different rainfall intensities and different rainfall durations in the vadose zone are shown in *Figure 8*.

*Figure 8* shows the downward migration of moisture in the vadose zone for different rainfall intensities. The hydraulic heads become increasingly concentrated in the vertical direction below the rainfall area as the rainfall time increases. The water flow usually moves vertically between the rainfall area and the groundwater table, and water infiltration in the vertical is much quicker than the percolation in the horizontal.

Contour plots of moisture content show the water infiltration process and the moving of wetting front. The figures showing the moving of the wetting front are presented in *Figure 9* for rainfall durations of 5, 20, 30 min and 15 min after the rainfall event respectively. The figure shows the distribution of moisture content within the vadose zone during a rainfall event. The red solid line represents the position of wetting front, at which the moisture content is approximately 20%. In addition, the movement of the wetting front shows a semi-oval shaped outward expansion. It can be obtained that for a rainfall duration of 29 min, the penetration distance of the water flow in vertical is about 50 cm, while the penetration distance in horizontal is only about 12 cm. This means the


http://www.aloki.hu ● ISSN 1589 1623 (Print) ● ISSN 1785 0037 (Online)
DOI: http://dx.doi.org/10.15666/aeer/1704_78377853

vertical penetration of water flow is much larger than the horizontal penetration, which causes the differences of gas expansion and compression in the vertical and horizontal directions. The unevenly moving of wetting front in directions is one of the causes of complicated gas migration and gas pressure changes.

Water flow infiltration rate ($q_i = dL_i/dt$, $i$ = x, z) in the vertical and horizontal directions can be derived from the distance moved by a moisture peak at different times, shown in *Figure 10* (line a and b). In addition, the surface infiltration flux is 78 cm/h. From Darcy's law, the rate of water flow infiltration can be calculated. At the sand surface:

$$R = -K_{w0}\left(\frac{h_1 - h_0}{\Delta z} - 1\right) \quad \text{(Eq.1)}$$

where $h_0$ and $K_{w0}$ are the hydraulic head and infiltration rate of the surface node respectively. The calculation results from Darcy's law are shown in *Figure 10* (line c).

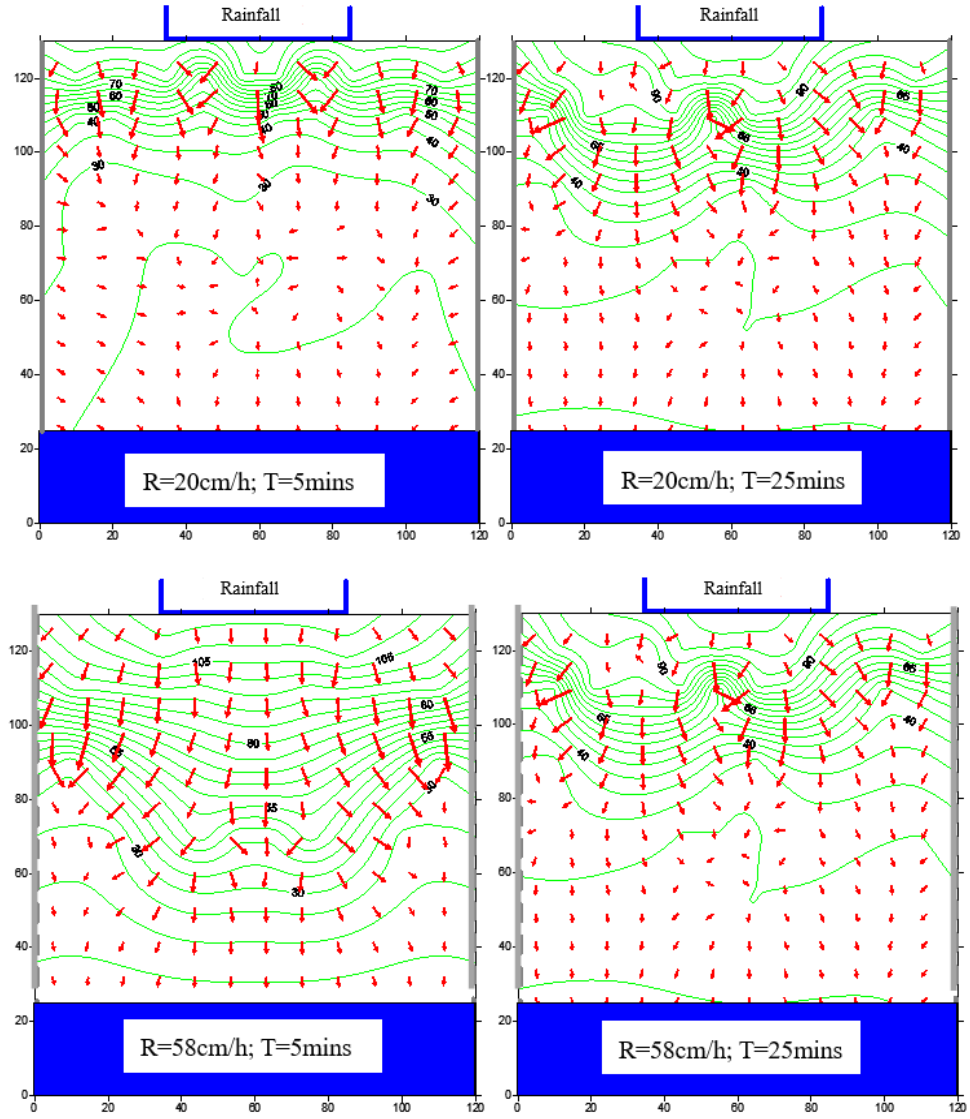


***Figure 8.*** *Distributions of hydrodynamic field for different rainfall intensities and different rainfall durations (unit of hydrodynamic field: cm)*


http://www.aloki.hu ● ISSN 1589 1623 (Print) ● ISSN 1785 0037 (Online)
DOI: http://dx.doi.org/10.15666/aeer/1704_78377853

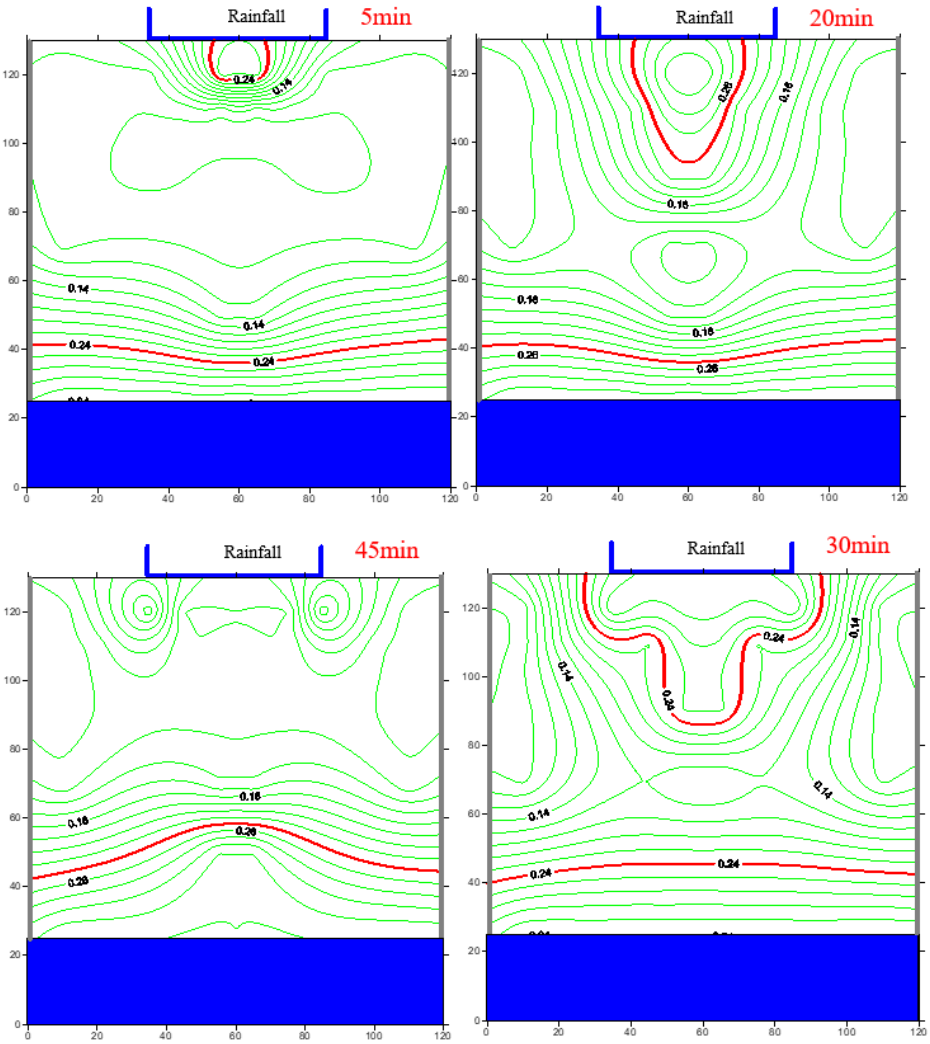


***Figure 9.*** *Distributions of moisture content within the vadose zone at different times after the onset of rainfall (the rainfall duration is 30 min)*

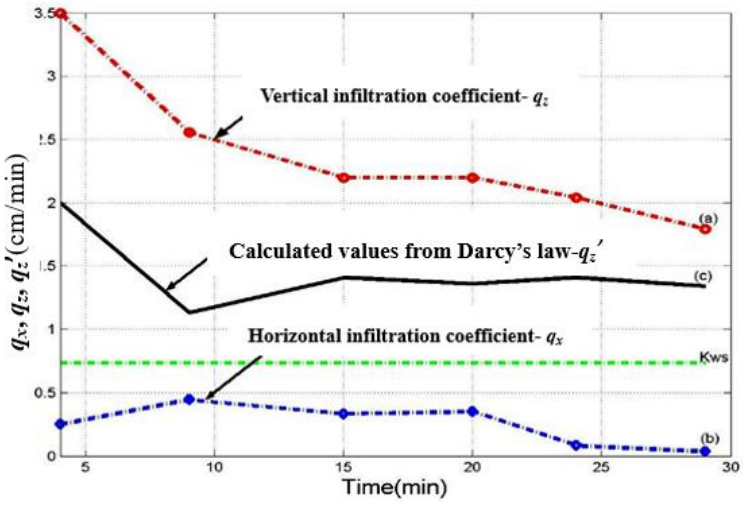


***Figure 10.*** *Time series for the rainfall infiltration rates*


http://www.aloki.hu ● ISSN 1589 1623 (Print) ● ISSN 1785 0037 (Online)
DOI: http://dx.doi.org/10.15666/aeer/1704_78377853

From *Figure 10,* we can see that water infiltration rate in the vertical ($q_z$) is significantly greater than that in the horizontal ($q_x$), that is $q_z >> q_x$. The calculated vertical infiltration rate from Darcy's law (*Fig. 10,* line c) is in accordance with the changing vertical infiltration rate derived from the movement of wetting front (*Fig. 10,* line a), but much larger. Early in the rainfall event, the flow infiltration rate is significantly greater than the saturated hydraulic conductivity $K_{ws}$. As the vadose zone soil porosity gradually become saturated, the vertical infiltration rate decreases, ultimately tending to the saturated hydraulic conductivity $K_{ws}$. The horizontal infiltration rate is much smaller throughout the rainfall event, and eventually tends to zero (*Fig. 10,* line b).

### *Distributions of moisture content in the central profile at X = 60cm*

Negative pressure (matric potential) varies with moisture content. So the changes of negative pressure are a useful mean of indirect measurement of moisture content in the vadose zone. Water column height (in cm) is used to represent the values of the negative pressure. The changes of negative pressure with depths under conditions of different rainfall intensities and rainfall durations are shown in *Figures 11* and *12*.

### *The relationship between the gas phase and the water phase*

Soil pores in the vadose zone are filled with either water or gas, so moisture migration resulting from rainfall infiltration is actually a mutual displacement process between the water and gas phases. The changes in moisture content cause the changes in gas pressure, while the negative pressure (matric potential) varies with moisture content, so there is a close relationship between air pressure, moisture content and negative pressure. The research of the relationship is important to understand the mechanisms of water and air migration in the vadose zone.

The time series of air pressure and negative pressure under conditions of different rainfall intensities are shown in *Figure 13*.

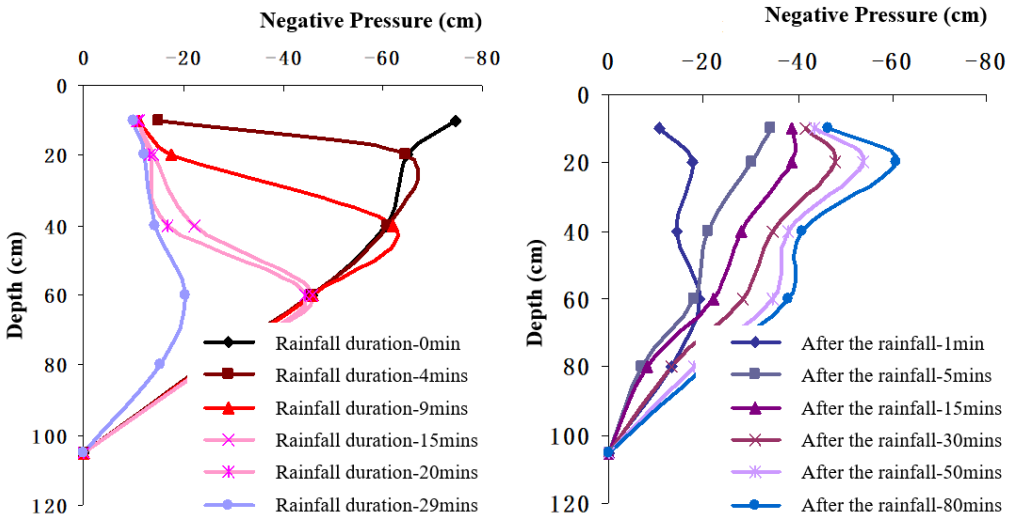


***Figure 11.*** *Changes of negative pressure with depths in the vadose zone for a rainfall intensity of 20 cm/h*


http://www.aloki.hu ● ISSN 1589 1623 (Print) ● ISSN 1785 0037 (Online)
DOI: http://dx.doi.org/10.15666/aeer/1704_78377853

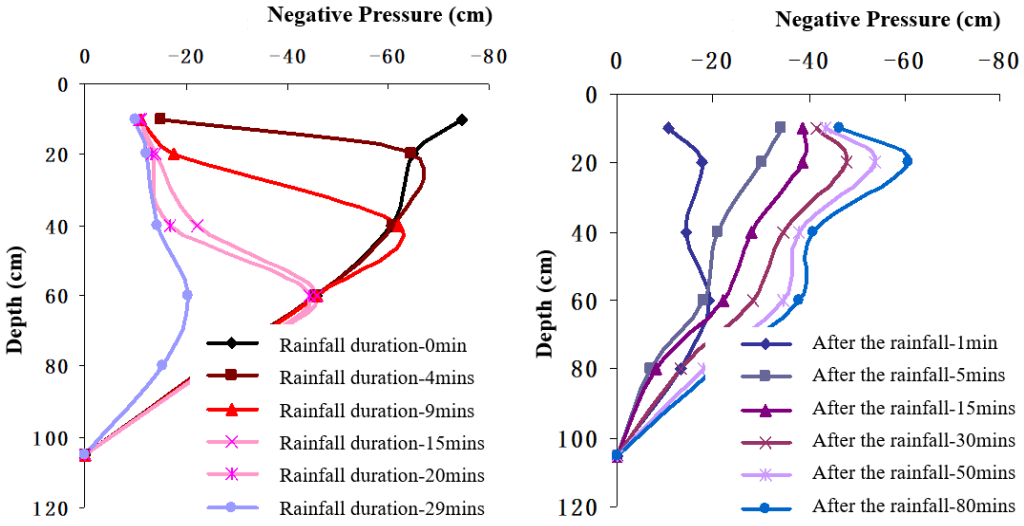


***Figure 12.*** *Changes of negative pressure with depths in the vadose zone for a rainfall intensity of 78 cm/h*

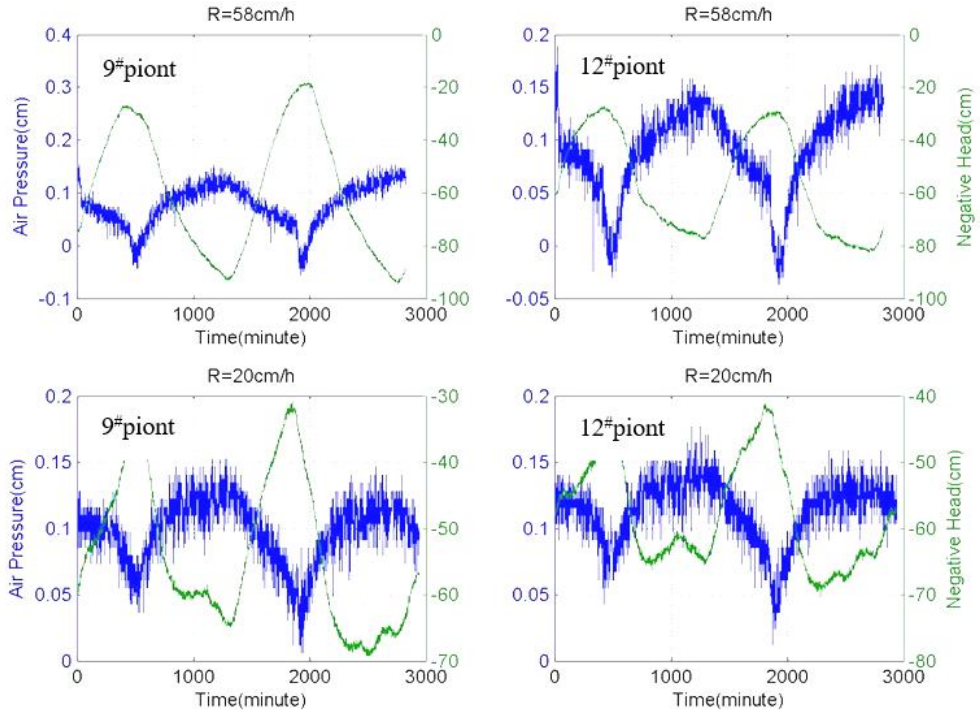


***Figure 13.*** *Time series of gas pressure and negative gas pressure for different pressure measuring points under different rainfall intensities*

## *How the gas phase blocks water infiltration*

The impact of the gas on the moisture migration. The mutual displacement relationship between the water phase and gas phase in the vadose zone is an important


http://www.aloki.hu ● ISSN 1589 1623 (Print) ● ISSN 1785 0037 (Online)
DOI: http://dx.doi.org/10.15666/aeer/1704_78377853

aspect of rainfall infiltration processes, and the blocking effect of the gas phase on water infiltration is particularly important. Using the groundwater recharge rate obtained from the rainfall infiltration experiments, Darcy's law can be expressed as the following equation:

$$q = -K_i\left(\frac{h_i - h_{i-1}}{\Delta z} - 1\right) \quad \text{(Eq.2)}$$

where $h_i$ and $h_{i-1}$ are the hydraulic head values for adjacent nodes near the groundwater table.

The unsaturated permeability coefficient *K(h)* can be obtained from *Equation 2*. The changes of *K(h)* with the pressure at node i are shown in *Figure 14*.

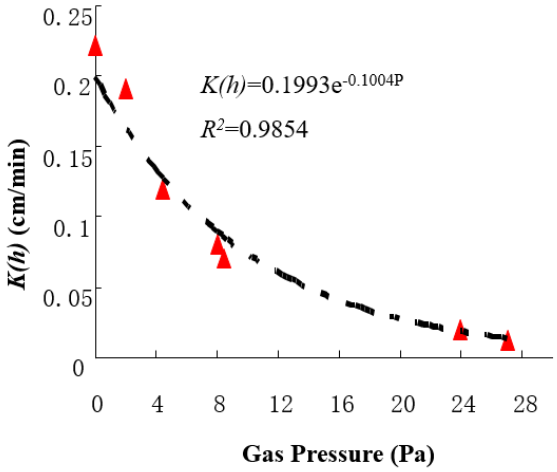


***Figure 14.*** *The relationship between the unsaturated permeability coefficient K(h) and gas pressure*

The response time of rainfall recharge. Define the response time of rainfall recharge as the period between the time at which the rainfall infiltrates into the vadose zone to the time at which the infiltrated water begins to recharge groundwater. This response time is closely related to rainfall duration, vadose zone lithology and structure, surface vegetation cover and groundwater depth. The changes of the response time under different rainfall intensities conditions are depicted in *Figure 15*.

## Discussion

### *Changes of the aerodynamic field under different boundaries*

From *Figures 2* and *3,* it is found that the high pressure center, where the gas pressure increases quickly and the gas compression degree is the highest, is located just below the rainfall area, but not close to the groundwater table whether under the gas insulation boundary or free exhaust boundary. When the gas pressure increases to a critical level, the gas begin to escape to surroundings or even break through the overlying water layer to escape out of the sand surface as a result of the pressure gradient. Under gas insulation conditions, the gas cannot escape from the sides, and so


http://www.aloki.hu ● ISSN 1589 1623 (Print) ● ISSN 1785 0037 (Online)
DOI: http://dx.doi.org/10.15666/aeer/1704_78377853

is eventually released from the sand surface. And the maximum pressure of the compressed gas is about 38 Pa after 29 min rainfall (*Fig. 4*). The gas movement is mainly in vertical. Under the free exhaust condition, the gas escapes from both sides of the tank and exchanges with the air outside exhibiting significant horizontal movement besides vertical movement. The maximum gas pressure is about 32 Pa after 29 min rainfall (*Fig. 4*).

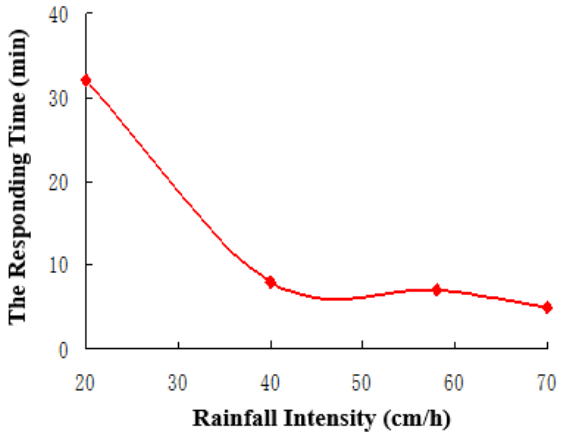


***Figure 15.*** *The changes of the response time under different rainfall intensities conditions*

From *Figure 4,* it can be seen that the maximum pressure is larger under the gas insulation condition than that under the free exhaust condition during rainfall infiltrating. Almost at the end time of the rainfall, the gas pressure reaches a critical value, after which the gas breaks through the overlying water layer and escapes, causing the pressure to reduce rapidly. After rainfall (from 40 to 180 min), the maximum profile pressure decreases much more rapidly under gas insulation condition than that under free exhaust boundary condition. In addition, the pressure values under gas insulation condition keep lower than that under free exhaust boundary condition after rainfall. The above results demonstrate that the degree of gas compression under the gas insulation condition is much greater than that under the free exhaust condition. The boundary has a significant influence on the gas migration in the vadose zone.

### *Changes of the gas pressure with the depth*

The gas pressure fluctuates strongly but approximately follows an "S" type with the depth from the surface to the bottom of the vadose zone either under a gas exhaust boundary or a gas insulation boundary. The difference is the location of the lower turning point. The location is at 60 cm under a gas exhaust boundary while it is at 20 cm under a 20 cm. The "S" type relationship between the gas pressure and depth divides the vadose zone into three zones. Zone I (at about 0–20 cm) is the gas escaping zone, where is close to the sand surface. The gas pressure in this zone decreases with the depth very slowly and reaches a minimum value at the depth of 20 cm. This is because this area reaches near-saturated in a comparatively short time during a rainfall event and the gas is quickly displaced by water. Zone II (at about 20-40 cm for gas insulation boundary; at about 20-60 cm for gas exhaust boundary) is the gas fluctuating zone. In this zone, the gas pressure increases quickly with the depth and reaches a maximum value at the


http://www.aloki.hu ● ISSN 1589 1623 (Print) ● ISSN 1785 0037 (Online)
DOI: http://dx.doi.org/10.15666/aeer/1704_78377853

depth of 40 cm (gas insulation boundary) or 60 cm (gas exhaust boundary). The maximum value decreases with the rainfall intensity. The reason is that the infiltrating flow advances rapidly in this zone, resulting in great changes in moisture content. The sustained infiltrating flow causes the gas resistance. And the downward movement of wetting front causes the gas compressed, so the gas cannot dissipate in time. Zone III (40–80 cm for gas insulation boundary; 60-80 cm for gas exhaust boundary) is the gas pressure fast-decreasing zone. In this zone, the gas pressure decreases with the depth. The flow tends to be steady due to the large infiltration distance and the reduced infiltration rate. Gas here slowly dissipates and escapes in the effect of the wetting front. Only a small amount of gas is transported to the groundwater table. The turning point illustrates that the gas movement does not only occur in the vertical direction but also in the horizontal direction. The turning point is where the gas is compressed and dissipated. The increase of gas pressure prevents the water from infiltrating and causes a lower hydraulic conductivity.

### *Changes of gas pressure at typical points*

*Figure 6* shows that the gas pressure fluctuates with time continuously around a mean value, exhibiting peaks and troughs. This is because the water infiltration causes gas to be constantly compressed during rainfall events. The increase in pressure causes the gas to break through the overlying water layer, which forms a pore channel. Then the pressure begins to decay rapidly and the pore channel is quickly re-occupied by water. This process repeats in the whole infiltration process, so the gas pressure in the vadose zone is not increasing or decreasing continuously, but in a state of fluctuation. The shape of the gas pressure time series curve shows that the changes of gas pressure in the vadose zone is similar with the fluctuations of the atmospheric pressure (Li, 2010). Pore channels form in the vadose zone and connect with the outside atmosphere, so the gas pressure changes are primarily related to the ambient atmospheric fluctuations. This result is consistent with the phenomenon described by Buckingham (1904), who considered that fluctuations in gas pressure in the vadose zone were related to changes in the near-surface atmospheric pressure. Massmann (1992) explained the near-surface atmospheric pressure fluctuations in detail. Massmann believed that the main causes of it were firstly the effect of heat conduction and gravity, and secondly the regional scaled weather conditions.

### *Distributions of moisture content in the central profile at X = 60 cm*

The results (*Figs. 11* and *12*) show that saturation state can be reached near the surface in a short period of time. At the onset of a rainfall, the moisture content is approximately the saturated moisture content and the negative pressure head is small. As the rainfall continues, the water-gas front moves downwards and the moisture content increases and the negative pressure head decreases. After the rainfall event, groundwater in the vadose zone is transported downwards under the influence of gravity. The negative pressure shows the trend of larger values at the lower depth and smaller values at the deeper depth.

### *Analysis of the relationship between the gas phase and the water phase*

The results (*Fig. 13*) show that the air pressure and negative pressure fluctuates with time: the negative pressure increases (negatively) with the air pressure increases, and


http://www.aloki.hu ● ISSN 1589 1623 (Print) ● ISSN 1785 0037 (Online)
DOI: http://dx.doi.org/10.15666/aeer/1704_78377853

vice versa. The increase in gas pressure at a point in the unsaturated zone indicates the entry of gas into pores near that point and the discharge of water from the pores. This corresponds to a decrease in the moisture content at that point, and a consequent increase in negative pressure. Similarly, a decrease in pressure indicates the entry of water into a pore near that point, following the discharge of gas from the pore, which corresponds to a decrease in negative pressure because of the increase in moisture content.

### *Analysis of how the gas phase blocks water infiltration*

The curve in *Figure 14* shows that the unsaturated permeability coefficient varies with gas pressure following the empirical relationship ($K(h) = 0.1993e^{-0.1004P}$). It is clear that the increase of the gas pressure results in the reducing of the unsaturated permeability coefficient during a rainfall event. It illustrates that increasing pressure will strongly attenuate the flow infiltration rate. For example, when the gas pressure reaches 270 Pa, the unsaturated permeability coefficient of water decreases from 0.22 cm/min to 0.03 cm/min. The effect of the gas phase on the unsaturated permeability coefficient gradually becomes weakened with the gas pressure increases, and the curve becomes flattened. Although this relationship does not provide a clear quantification of the relationship between gas pressure and the unsaturated permeability coefficient, it does clearly demonstrate how the increasing pressure has a blocking effect on the water flow, resulting in the water infiltration rate reduction.

*Figure 15* shows that the response time decreases as rainfall intensity increases. The greater the rainfall intensity, the faster the flow infiltration rate, and the shorter time taken for the flow to reach the groundwater table. Although rainfall infiltration leads to gas compression and creates a partial block to the flow, this does not completely prevent the flow, and the response time is mainly determined by the magnitude of the rainfall intensity.

## Conclusions

In order to obtain the mechanism of water infiltrating into an air block area in the vadose zone under conditions of different rainfall intensities and boundaries, a two-dimensional sand tank is made and lots of experiments are conducted. From the data analysis, the following conclusions can be drawn:

(1) The boundary has a significant influence on the gas pressure. The gas moves primarily in the vertical direction under a gas insulation boundary. However, the gas exhibits significant lateral diffusion besides vertical movement under a gas exhaust boundary. When the gas pressure reaches to a sufficiently high value, the gas escapes to the surroundings even break through the overlying water layer.

(2) The gas pressure fluctuates strongly but approximately follows an “S” type with the depths. So the vadose zone can be divided into three zones: Zone I is the gas escaping zone; Zone II is the gas pressure fluctuating zone; Zone III is the gas pressure fast-decreasing zone.

(3) The unsaturated permeability coefficient varies with gas pressure following an empirical relationship. The block effect of the gas phase on the unsaturated permeability coefficient gradually becomes weakened with the gas pressure increases.


http://www.aloki.hu ● ISSN 1589 1623 (Print) ● ISSN 1785 0037 (Online)
DOI: http://dx.doi.org/10.15666/aeer/1704_78377853

**Acknowledgements.** This research was funded by The National Natural Science Foundation of China (41702285, 41372260) and the Scientific Starting Project of High-Level Talents of North China University of Water Resources and Electric Power (201702002) and the Geological Survey Projects Foundation of Institute of Hydrogeology and Environmental Geology (SK201505).

## REFERENCES

[1] Buckingham, E. (1904): Contributions to our knowledge of the aeration of soils. – Science 25: 5-52.
[2] Du, C., Yu, J., Wang, P. et al. (2017): Analysing the mechanisms of soil water and vapour transport in the desert vadose zone of the extremely arid region of northern China. – Journal of Hydrology S0022169417306583.
[3] Ghosh, S., Pratihar D. K., Maiti, B. et al. (2012): Identification of flow regimes using conductivity probe signals and neural networks for counter-current gas–liquid two-phase flow. – Chemical Engineering Science 84: 417-436.
[4] Grismer, M. E., Orang, M. N., Clausitzer, V., Kinney, K. (1994): Effects of air compression and counter flow on infiltration into soils. – Journal of Irrigation & Drainage Engineering 120: 775-795.
[5] Herrada, M. A., Gutiérrez-Martin, A., Montanero, J. M. (2014): Modeling infiltration rates in a saturated/unsaturated soil under the free draining condition. – Journal of Hydrology 515: 10-15.
[6] Jarrett, A. R., Friton, D. D. (1978): Effect of entrapped soil air on infiltration. – Transactions of the ASAE 21(5): 901-906.
[7] Jie, Z., Tong-Chun, H., Hong-Qiang, D. et al. (2013): Analysis model for rainwater infiltration considering gas resistance under stratified assumption. – Yantu Gongcheng Xuebao/Chinese Journal of Geotechnical Engineering 35(12): 2219-2225.
[8] Lei, L., Bing, L., Qiang, X. (2009): Prediction analysis of water infiltration effect on landfill gas transport. – Physical and Numerical Simulation of Geotechnical Engineering 15: 43-45.
[9] Lei, Z. D., Yang, S. H., Xie, C. S. (1988): Soil Water Dynamics. – Tsinghua University Press, Beijing, pp. 21-22.
[10] Lu, T. X., Biggar, J. E., Nielsen, D. R. (1994): Water movement in glass bead porous media: 2. Experiments of infiltration and finger flow. – Water Resources Research 30: 3283-3290.
[11] Li, J., Zhao, J., Wang, S. (2015): Gas–liquid two-phase flow in a mini-channel with water infiltration continuously along the flow direction. – International Journal of Green Energy 12(3): 8.
[12] Li, Y. L. (2010): Simulation Study of Two-Phases (Water and Air) Flow in Unsaturated Zone under Infiltration Condition. – Chang'an University, Xi'an, China.
[13] Massmann, J., Farrier, D. (1992): Effects of atmospheric pressure on gas transport in the vadose zone. – Water Resources Research 28(3): 777-791.
[14] Min, L., Shen, Y., Pei, H. et al. (2018): Water movement and solute transport in deep vadose zone under four irrigated agricultural land-use types in the North China Plain. – Journal of Hydrology S0022169418301136.
[15] Peck, A. J. (1965a): Moisture profile development and air compression during water uptake by bounded porous bodies: 2. Horizontal columns. – Soil Science 100: 333-340.
[16] Peck, A. J. (1965b): Moisture profile development and air compression during water uptake by bounded porous bodies: 3. Vertical columns. – Soil Science 100: 44-51.
[17] Peng, S., Chen, J. J., Wang, J. S. (2002): Two-phase flow in soil vadose zone. – Acta Pedologica Sinica 39(4): 505-511.
[18] Touma, J., Vauclin, M. (1986): Experimental and numerical analysis of two-phase infiltration in a partially saturated soil. – Transport in Porous Media 1: 27-55.


http://www.aloki.hu ● ISSN 1589 1623 (Print) ● ISSN 1785 0037 (Online)
DOI: http://dx.doi.org/10.15666/aeer/1704_78377853

[19] Wang, Z., Feyen, J., Nielsen, D. R., Genuchten, M. T. V. (1997): Two-phase flow infiltration equations accounting for air entrapment effects. – Water Resources Research 33: 2759-2767.
[20] Xiao, J., Luo, X., Feng, Z. et al. (2018): Using artificial intelligence to improve identification of nanofluid gas–liquid two-phase flow pattern in mini-channel. – AIP Advances 8(1): 015123.
[21] Zhao, G. Z. (2011): Study on Transformation Mechanism of Vadose Zone Water-Groundwater in the Wind-blown Sand Area of the Ordos Basin. – Chang'an University, Xi'an, China.


http://www.aloki.hu ● ISSN 1589 1623 (Print) ● ISSN 1785 0037 (Online)
DOI: http://dx.doi.org/10.15666/aeer/1704_78377853